

A NUMERICAL INVESTIGATION OF INERTIA INFLUENCE ON SMD FLUIDS FLOWING AROUND A CONFINED CYLINDER

Daniel Dall'Onder dos Santos, dallonder@mecanica.ufrgs.br

Lober Hermany, hermany@mecanica.ufrgs.br

Sérgio Frey, frey@mecanica.ufrgs.br

Laboratory of Computational and Applied Fluid Mechanics (LAMAC) – Department of Mechanical Engineering – Federal University of Rio Grande do Sul – Rua Sarmento Leite, 425 – 90050-170 – Porto Alegre, RS, Brazil

Mônica F. Naccache, naccache@puc-rio.br

Department of Mechanical Engineering, Pontifícia Universidade Católica do Rio de Janeiro
Rua Marquês de São Vicente 225 – 22453-900 – Rio de Janeiro, RJ, Brazil

Abstract. *The current article aims to perform stabilized finite element approximations for inertia flows of SMD (Souza Mendes and Dutra, 2004) viscoplastic materials. The viscoplastic model is approximated by a multi-field Galerkin least squares method in extra-stress, pressure and velocity. This methodology does not need to satisfy the compatibility conditions arisen from finite element sub-spaces for extra-stress–velocity and pressure–velocity. That is accomplished by adding mesh-dependent terms, which are functions of residuals of flow governing equations, to the classical Galerkin formulation. Numerical simulations of the flow around a cylinder inside a planar channel are carried out. To evaluate the influence of yield stress limit and inertia on material yield surfaces, the dimensionless flow-rate U^* is investigated from 0.01 to 1.0 and a rheological definition for the Reynolds number from 1.0 to 50. The results generated in this work reassure the fine stability features of the GLS formulation and the adequacy of the SMD equation in describing the stress-strain relation for non-linear viscoplastic fluid flows.*

Keywords: *viscoplasticity; regularized viscoplastic models; SMD fluid; multi-field Galerkin least-squares method.*

1. INTRODUCTION

During the past several decades the emphasis in rheology and continuum mechanics has been in one-phase materials with particular attention to polymer solutions and melts. Slurries, pastes and suspensions, frequently, encountered in industrial applications, have received less attention than they deserve. Many of these materials have an yield-stress, a critical value of stress below which they do not flow; they are usually called viscoplastic materials. Another examples of materials that fall in this category are xanthan gum, drilling mud, cement, paints and grease.

The present article concerns stabilized finite element approximations for non-linear viscoplastic materials flowing under inertia influence. The employed material equation is the viscoplastic one introduced by Souza Mendes and Dutra (2004) – henceforth named SMD fluid. This model is approximated by a multi-field Galerkin least squares method in terms of extra-stress, pressure and velocity. This methodology – introduced by Hughes *et al.* (1986), for the Stokes problem, and later extended to mixed and multi-field Navier-Stokes equations in Franca and Frey (1992) and in Behr *et al.* (1993), respectively – does not need to satisfy the compatibility conditions arisen from finite element sub-spaces for extra-stress–velocity and pressure–velocity fields. It enhances the stability of the classical Galerkin method adding mesh-dependent terms, which are functions of the residuals of flow governing equations, evaluated element-wise.

Numerical simulations of the flow around a cylinder inside a planar channel are carried out. In order to evaluate the influence of yield stress and inertia on yield surfaces of viscoplastic materials, the dimensionless flow-rate U^* is varied from 0.01 to 1.0 and a new definition for the Reynolds number – introduced by Souza Mendes (2007) – is ranged from 1.0 to 50, with the SMD dimensionless number J set as 10^4 . In all computations, a combination of equal-order bilinear finite element interpolations are used to approximate the primal variables of the problem, thence violating the involved compatibility conditions. The results generated in this work proved to be physical meaningful and are in accordance to the viscoplastic literature

2. MECHANICAL MODELING

Assuming an isothermal flow around a cylinder inside a planar channel, it suffices to solve only the mass and linear momentum balance equations, since the Cauchy stress tensor is a symmetric one – thence automatically satisfying the balance of angular momentum (Astarita and Marrucci, 1974). For incompressible fluids, the continuity equation may be written as

$$\text{div } \mathbf{u} = 0 \tag{1}$$

where \mathbf{u} is the fluid velocity field.

Assuming the stress tensor \mathbf{T} decomposition in a spherical and deviatoric portions, $\mathbf{T} = -p\mathbf{I} + \boldsymbol{\tau}$ – with p representing a non thermodynamic pressure, \mathbf{I} the unity tensor, and $\boldsymbol{\tau}$ the extra-stress tensor, the momentum balance equation for steady flows may be stated as (Astarita and Marrucci, 1974)

$$\rho(\nabla \mathbf{u})\mathbf{u} + \nabla p - \text{div } \boldsymbol{\tau} = \mathbf{f} \quad (2)$$

with ρ representing the fluid density and \mathbf{f} the body force vector.

In inelastic non-Newtonian fluid flows, the extra-stress tensor may be related to fluid kinematics by a generalization of Newton law for viscosity, the so-called generalized Newtonian (GNL) law (Bird *et al.*, 1987),

$$\boldsymbol{\tau} = 2\eta(\dot{\gamma})\mathbf{D} \quad (3)$$

in which $\eta(\dot{\gamma})$ is a shear-rate-dependent viscosity, a function of the second invariant of the tensor \mathbf{D} ,

$$\dot{\gamma} = (2 \text{tr } \mathbf{D}^2)^{1/2} \quad (4)$$

In the present work, the employed viscoplastic function is the one recently introduced by Souza Mendes and Dutra (2004) for non-linear viscoplastic materials. According the SMD model, the shear stress is expressed by

$$\boldsymbol{\tau} = (1 - \exp(-\eta_0 \dot{\gamma} / \tau_0))(\tau_0 + K \dot{\gamma}^n) \quad (5)$$

where τ_0 is the yield stress limit of the material, K is the consistency index, η_0 is the Newtonian viscosity for very low values of the shear rate, n is the power-law exponent – that controls the shear-thinning of the viscosity when the material starts to flow – and τ is the magnitude of the extra-stress tensor,

$$\tau = (1/2 \text{tr } \boldsymbol{\tau}^2)^{1/2} \quad (6)$$

From Eq. (4) and (5), the SMD viscosity function may be written as

$$\eta(\dot{\gamma}) = (1 - \exp(-\eta_0 \dot{\gamma} / \tau_0)) \left(\frac{\tau_0}{\dot{\gamma}} + K \dot{\gamma}^{n-1} \right) \quad (7)$$

The Eq.(5) may be written in a non-dimension form through the introduction of the jump number J , a SMD dimensionless parameter, that gives the relative measure of the shear rate jump that occurs when $\tau = \tau_0$,

$$J \equiv \frac{\dot{\gamma}_1 - \dot{\gamma}_0}{\dot{\gamma}_0} = \frac{\eta_0 \tau_0^{(1-n)/n}}{K^{1/n}} \quad (8)$$

where $\dot{\gamma}_0$ is the shear rate at the end of the Newtonian-like behavior – in which the viscosity is equal to η_0 – and $\dot{\gamma}_1$ corresponds to the shear rate at the beginning of the shear- thinning region on the SMD flow curve – see, for details, Souza Mendes *et al.* (2007). Hence, the SMD function may be written in a dimensionless form as

$$\boldsymbol{\tau}^* = (1 - \exp(-(J+1)\dot{\gamma}^*)) (1 + \dot{\gamma}^{*n}) \quad (9)$$

3. FINITE ELEMENT APPROXIMATION

The problems considered herein are defined on a bounded open domain $\Omega \subset \mathfrak{R}^2$ with a polygonal or polyhedral boundary Γ , formed by the union of Γ_g – the portion of Γ wherein Dirichlet conditions are imposed – and Γ_h – the boundary portion subjected to Neumann conditions. A partition Ω_h of $\bar{\Omega}$ into finite elements is performed in the usual way, namely no overlapping is allowed between any two elements, the union of all element domains Ω_k reproduces $\bar{\Omega}$ and a combination of triangles and quadrilaterals for the two-dimensional case can be accommodated (Ciarlet, 1978).

As usual, $L_2(\Omega)$, $L_2^0(\Omega)$, $H^1(\Omega)$ and $H_0^1(\Omega)$ stand for Hilbert and Sobolev functional spaces, respectively, as follows,

$$\begin{aligned}
 L_2(\Omega) &= \{q \mid \int_{\Omega} q^2 d\Omega < \infty\} \\
 L_2^0(\Omega) &= \{q \in L_2(\Omega) \mid \int_{\Omega} q d\Omega = 0\} \\
 H^1(\Omega) &= \{v \in L_2(\Omega) \mid \partial_{x_i} v \in L_2(\Omega), \quad i=1, N\} \\
 H_0^1(\Omega) &= \{v \in H^1(\Omega) \mid v=0 \text{ on } \Gamma_g, \quad i=1, N\}
 \end{aligned} \tag{10}$$

From Eq. (1)-(4) and (7), a multi-field boundary-value problem for inertia steady flows of SMD viscoplastic fluids may be stated as,

$$\begin{aligned}
 \rho([\nabla \mathbf{u}]\mathbf{u}) + \nabla p - \operatorname{div} \boldsymbol{\tau} &= \mathbf{f} && \text{in } \Omega \\
 \boldsymbol{\tau} - 2(1 - \exp(-\eta_0(2\operatorname{tr} \mathbf{D}^2)^{1/2}/\tau_0))(\tau_0(2\operatorname{tr} \mathbf{D}^2)^{-1/2} + K(2\operatorname{tr} \mathbf{D}^2)^{(n-1)/2}) \mathbf{D}(\mathbf{u}) &= 0 && \text{in } \Omega \\
 \operatorname{div} \mathbf{u} &= 0 && \text{in } \Omega \\
 \mathbf{u} &= \mathbf{u}_g && \text{on } \Gamma_g^u \\
 \boldsymbol{\tau} &= \boldsymbol{\tau}_g && \text{on } \Gamma_g^{\boldsymbol{\tau}} \\
 [-p \mathbf{I} + \boldsymbol{\tau}] \mathbf{n} &= \mathbf{t}_h && \text{on } \Gamma_h
 \end{aligned} \tag{11}$$

where \mathbf{n} the outward unit vector, \mathbf{t}_h the stress vector, and the remaining variables are defined as previously.

The finite element approximation for the multi-field boundary-problem defined by Eq. (11) may be built employing the following finite element subspaces for extra stress ($\boldsymbol{\Sigma}^h$), velocity (\mathbf{V}^h) and pressure (P^h) fields,

$$\begin{aligned}
 \mathbf{V}^h &= \{\mathbf{v} \in H_0^1(\Omega)^N \mid \mathbf{v}|_K \in R_k(K)^N, \quad K \in \Omega^h\} \\
 \mathbf{V}_g^h &= \{\mathbf{v} \in H^1(\Omega)^N \mid \mathbf{v}|_K \in R_k(K)^N, \quad K \in \Omega^h, \quad \mathbf{v} = \mathbf{u}_g \text{ on } \Gamma_g\} \\
 P^h &= \{p \in C^0(\Omega) \cap L_2^0(\Omega) \mid p|_K \in R_l(K), \quad K \in \Omega^h\} \\
 \boldsymbol{\Sigma}^h &= \{\mathbf{S} \in C^0(\Omega)^{N \times N} \cap L_2(\Omega)^{N \times N} \mid S_{ij} = S_{ji}, \quad i, j = 1, N, \quad \mathbf{S}|_K \in R_m(K)^{N \times N}, \quad K \in \Omega^h\}
 \end{aligned} \tag{12}$$

with R_k , R_l and R_m denoting polynomial spaces of degree k , l and m , respectively. Based on these definitions, a multi-field Galerkin least-squares formulation for inertia flows of SMD fluids may be written as: given the functions of body force \mathbf{f} and Dirichlet and Neumann boundary conditions $\boldsymbol{\tau}_g$ and \mathbf{u}_g , and \mathbf{t}_h respectively, find the triple $(\boldsymbol{\tau}^h, p^h, \mathbf{u}^h) \in \boldsymbol{\Sigma}^h \times P^h \times \mathbf{V}_g^h$ such that

$$B(\boldsymbol{\tau}^h, p^h, \mathbf{u}^h; \mathbf{S}^h, q^h, \mathbf{v}^h) = F(\mathbf{S}^h, q^h, \mathbf{v}^h) \quad \forall (\mathbf{S}^h, q^h, \mathbf{v}^h) \in \boldsymbol{\Sigma}^h \times P^h \times \mathbf{V}_g^h \tag{13}$$

with

$$\begin{aligned}
 B(\boldsymbol{\tau}^h, p^h, \mathbf{u}^h; \mathbf{S}^h, q^h, \mathbf{v}^h) &= [2(1 - \exp(-\eta_0(2\operatorname{tr} \mathbf{D}^2)^{1/2}/\tau_0))(\tau_0(2\operatorname{tr} \mathbf{D}^2)^{1/2} + K(2\operatorname{tr} \mathbf{D}^2)^{(n-1)/2})]^{-1} \int_{\Omega} \boldsymbol{\tau}^h \cdot \mathbf{S}^h d\Omega \\
 &+ \int_{\Omega} \rho([\nabla \mathbf{u}^h]\mathbf{u}^h) \cdot \mathbf{v}^h d\Omega - \int_{\Omega} \boldsymbol{\tau}^h \cdot \mathbf{D}(\mathbf{v}^h) d\Omega - \int_{\Omega} p^h \operatorname{div} \mathbf{v}^h d\Omega + \int_{\Omega} \operatorname{div} \mathbf{u}^h q^h d\Omega + \epsilon \int_{\Omega} p^h q^h d\Omega - \int_{\Omega} \mathbf{D}(\mathbf{u}^h) \cdot \mathbf{S}^h d\Omega \\
 &+ \sum_{K \in \Omega^h} \int_{\Omega_K} (\rho[\nabla \mathbf{u}^h]\mathbf{u}^h + \nabla p^h - \operatorname{div} \boldsymbol{\tau}^h) \cdot (\alpha(\operatorname{Re}_K)(\rho[\nabla \mathbf{v}^h]\mathbf{u}^h + \nabla q^h - \operatorname{div} \mathbf{S}^h)) d\Omega + \delta \int_{\Omega} \operatorname{div} \mathbf{u}^h \operatorname{div} \mathbf{v}^h d\Omega \\
 &+ 2(1 - \exp(-\eta_0(2\operatorname{tr} \mathbf{D}^2)^{1/2}/\tau_0))(\tau_0(2\operatorname{tr} \mathbf{D}^2)^{1/2} + K(2\operatorname{tr} \mathbf{D}^2)^{(n-1)/2}) \beta \cdot \int_{\Omega} ([2(1 - \exp(-\eta_0(2\operatorname{tr} \mathbf{D}^2)^{1/2}/\tau_0))(\tau_0(2\operatorname{tr} \mathbf{D}^2)^{-1/2} + K(2\operatorname{tr} \mathbf{D}^2)^{(n-1)/2})]^{-1} \boldsymbol{\tau}^h - \mathbf{D}(\mathbf{u}^h)) \cdot ([2(1 - \exp(-\eta_0(2\operatorname{tr} \mathbf{D}^2)^{1/2}/\tau_0))(\tau_0(2\operatorname{tr} \mathbf{D}^2)^{-1/2} + K(2\operatorname{tr} \mathbf{D}^2)^{(n-1)/2})]^{-1} \mathbf{S}^h - \mathbf{D}(\mathbf{v}^h)) d\Omega
 \end{aligned} \tag{14}$$

and

$$F(\mathbf{S}^h, q^h, \mathbf{v}^h) = \int_{\Omega} \mathbf{f} \cdot \mathbf{v}^h d\Omega + \int_{\Gamma_h} \mathbf{t}_h \cdot \mathbf{v}^h d\Gamma + \sum_{K \in \Omega^h} \int_{\Omega_K} \mathbf{f} \cdot (\alpha(\operatorname{Re}_K)(\rho[\nabla \mathbf{v}^h]\mathbf{u}^h + \nabla q^h - \operatorname{div} \mathbf{S}^h)) d\Omega \tag{15}$$

where the grid Reynolds number Re_K and the stability parameters $\alpha(\operatorname{Re}_K)$ and δ are defined as in Franca and Frey (1992),

$$\alpha(\text{Re}_K) = \frac{h_K}{2|\mathbf{u}^h|_p} \xi(\text{Re}_K)$$

$$\xi(\text{Re}_K) = \begin{cases} \text{Re}_K, & 0 < \text{Re}_K < 1 \\ 1, & \text{Re}_K > 1 \end{cases} \quad (16)$$

$$\text{Re}_K = \frac{\rho h_K |\mathbf{u}^h|_p m_k}{4(1 - \exp(-\eta_0(2\text{tr} \mathbf{D}^2)^{1/2}/\tau_0))(\tau_0(2\text{tr} \mathbf{D}^2)^{-1/2} + K \dot{\gamma}^{n-1})}$$

$$m_k = \min\{1/3, 2C_k\}$$

and the stability parameter for the SMD equation β is defined as an arbitrary positive value according to Behr *et al.* (1993), and m_k is a positive scalar that takes in to account the the k -degree of the polynomial interpolations – see Franca and Frey (1992), for details.

4. NUMERICAL RESULTS

In this section, the multi-field GLS formulation defined by Eq. (13)-(16) has been employed to approximate SMD fluid flows around a cylinder kept between two parallel plates. The dimensionless parameters employed to characterize the flows are, first, the dimensionless flow rate U^* (see Souza Mendes *et al.*, 2007),

$$U^* = \frac{u_0}{\dot{\gamma}_1 L_c} \quad (17)$$

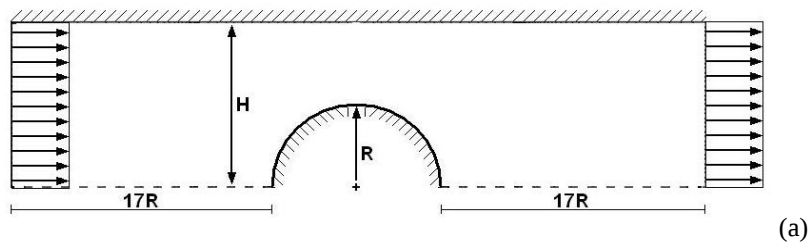
where u_0 is the flow rate at the channel inlet and the the characteristic length L_c is taken as the cylinder radius. Secondly, to account for inertia effects, the Reynolds number Re_{RH} , a dimensionless parameter based only on fluid properties (Souza Mendes, 2007),

$$\text{Re}_{RH} = \frac{\rho \dot{\gamma}_1^{n-1} L^2}{K} \quad (18)$$

and, finally, the jump number J introduced by Eq.(8). It is worth mentioning that Re_{RH} may be related to the usual Reynolds definition accounting for the shear-thinning of the viscosity (see, for instance, Jay *et al.*, 2001) by the expression (see Santos *et al.* (2010), for details)

$$\text{Re}_{PL} = \text{Re}_{RH} U^{*(2-n)} \quad (19)$$

Figure 1a schematically shows the employed boundary conditions in the numerical simulations: uniform parallel velocity u_0 at channel inlet and outlet, no-slip and impermeability on channel walls and on the cylinder surface, and symmetry conditions on the channel centerline ($\partial_2 u_1 = u_2 = \tau_{12} = 0$). The channel aspect ratio, i. e. the half of channel width (H) divided by the cylinder radius (R), is set as two. In order to guarantee fully-developed flow regions upstream and downstream of the cylinder, the mesh lengths either upstream or downstream of th cylinder are set equal to $17R$. After a mesh independence procedure that compares the dimensionless pressure drop for each consecutive mesh refinements, the selected mesh, with 11,584 bilinear Lagrangian (Q1) finite elements, presents an overall error less then 1% when compared to the next more refined mesh – see Fig.1b for a blown-up view around the cylinder of the selected mesh.



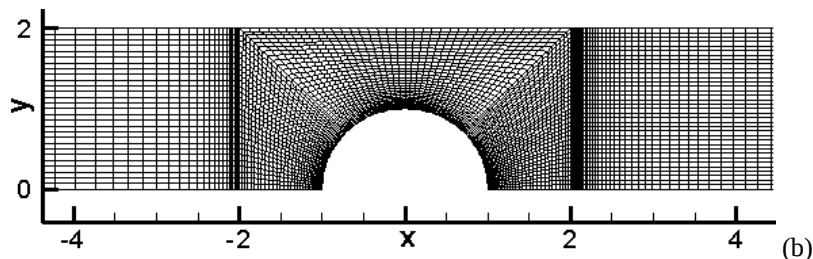


Figure 1. Flow around a cylinder: (a) the problem statement; (b) a blown-up view of the selected mesh.

The influence of yield stress effects on the development of yielded and unyielded regions (black zones) in inertia flows of SMD fluids is shown in Fig. 2, for $U^*=0.01-1.0$, $Re_{RH}=1.0$, $J=10^4$ and $n=0.5$. One may observe that all unyielded regions at the cylinder vicinity are strongly reduced as U^* grows – namely, the plug-flows upstream and downstream of the cylinder, the island over the cylinder equator and the tiny polar caps only visible in Fig. 2a, for $U^*=0.01$. Such kind of behavior may be explained by the decreasing of yield stress effects thanks to the increasing of U^* .

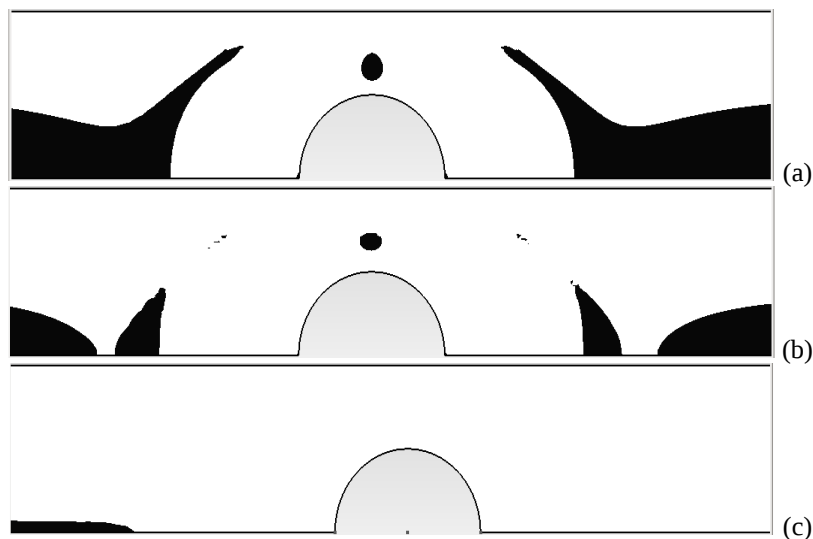


Figure 2. Yielded and unyielded regions, for $Re_{RH}=1.0$, $J=10^4$ and $n=0.5$: (a) $U^*=0.01$; (b) $U^*=0.1$; (c) $U^*=1.0$.

Fig. 3 shows the influence of yield stress on the shear-stress (Eq.(6)) profiles, along the rectified channel centerline S , for $Re_{RH}=1.0$, $J=10^4$ and $n=0.5$. It may be observed that the more U^* increases, the more shear stress increases, too. Besides, shear stress peaks occur over the cylinder (around $S=0$) and an asymmetrical profile pattern may be clearly verified for the highest value of the flow-rate ($U^*=1.0$). Both behaviors may be credited to the decreasing of the yield stress effect, owing to the increasing of U^* . In the first case, the decreasing of the yield stress effect – or, for a regularized viscoplastic fluid, of the viscous effect – leaves the flow subjected to higher values of shear stress. In second one, for the same reason, the flow becomes advective dominated with the decreasing of the yield stress effect.

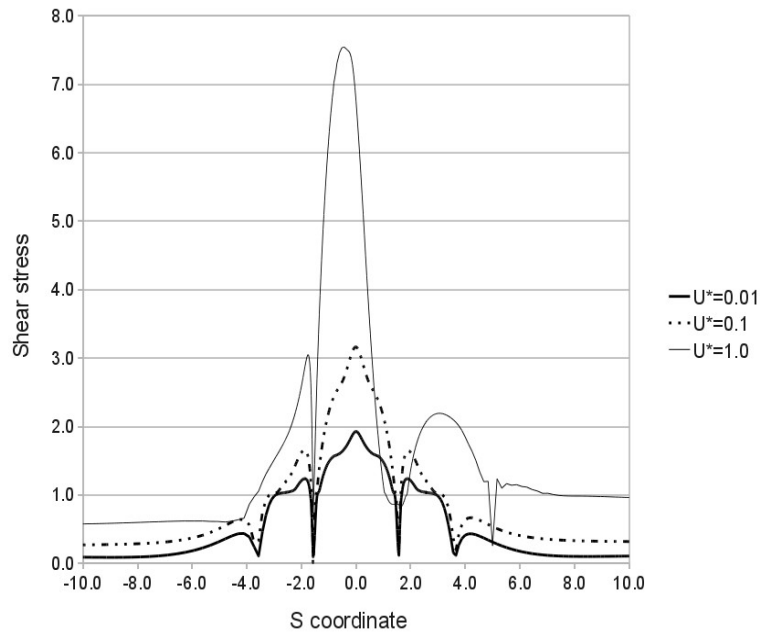


Figure 3. Longitudinal profile of shear stress, for $Re_{RH}=1.0$, $J=10^4$ and $n=0.5$ and $U^*=0.01-1.0$.

In Fig. 4 the investigation of the influence of inertia on SMD fluid dynamics is carried out, for $J=10^4$, $U^*=0.1$, $n=0.5$ and $Re_{RH}=1-50$. As expected, the more inertia effects increase the more the vortex size increases, too. It is worth observing that, due to the uncoupled way in which the Re_{RH} is defined, from flow kinematics, by Eq.(18), the increasing of Re_{RH} does not affect the material yielded stress, as observed in inertia flows parametrized by power-law Reynolds and Herschel-Bulkley numbers – see, for instance, Jay et al., 2001.

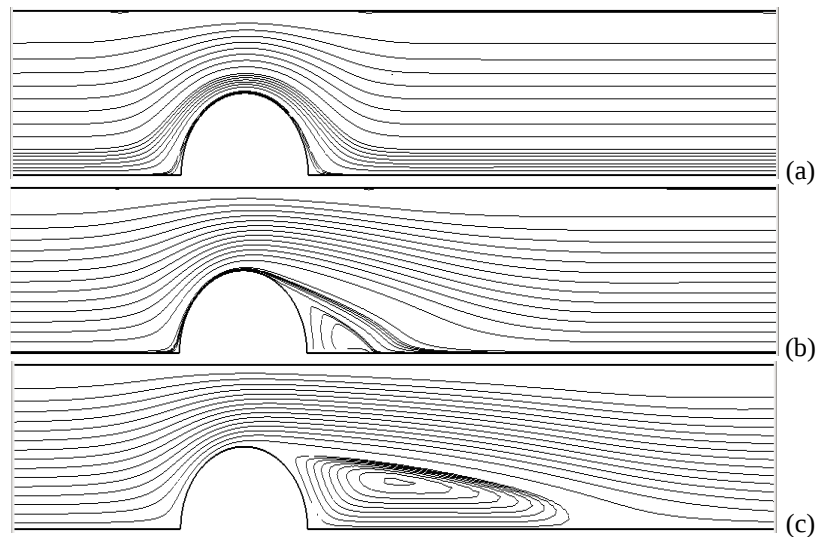


Figure 4. Streamlines for $J=10^4$, $U^*=0.1$ and $n=0.5$: (a) $Re_{RH}=1$; (b) $Re_{RH}=20$; (c) $Re_{RH}=50$.

Figure 5 shows the influence of inertia effects on shear stress profiles along rectified channel centerline, for $J=10^4$, $U^*=0.1$, $n=0.5$ and $Re_{RH}=1-50$. From the figure, the shear stress peaks over the cylinder surface significantly increase as Re_{RH} increases. In addition, the shear stress profiles present an asymmetrical pattern with the increasing of Re_{RH} , due to the flow being more advective dominated

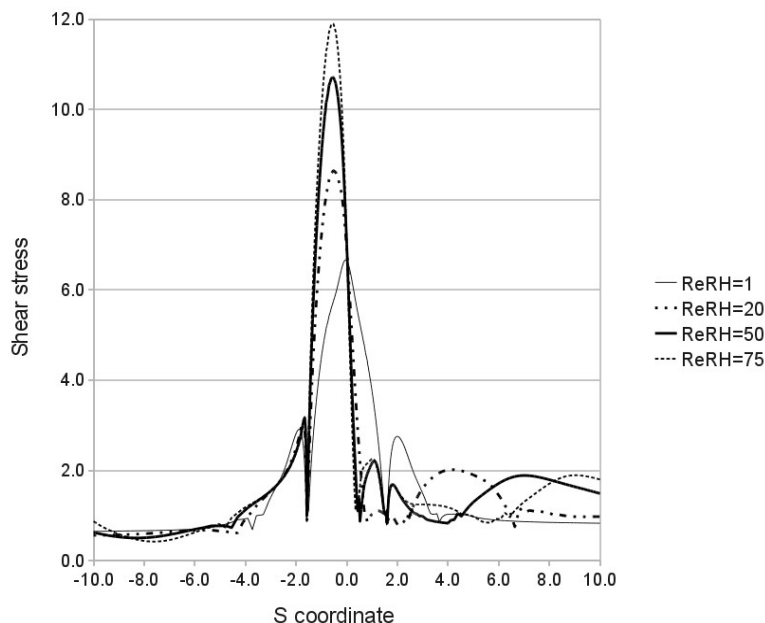


Figure 5. Shear stress along the S coordinate varying the rheological Reynolds number.

5. FINAL REMARKS

In this article, some numerical simulations of inertia flows of viscoplastic fluids have been undertaken. The viscoplastic fluid is the one introduced by Souza Mendes and Dutra (2004) and the mechanical model is approximated via a multi-field Galerkin least-squares method in extra-stress, pressure and velocity. Due to the good stability features of the GLS method, all computations have employed a combination of equal-order bilinear Lagrangian finite elements and high Reynold flows have been stably achieved. The numerical results have evidenced the strong influence of yield stress effects on the size of unyielded material regions, and the inertia ones proved to play a relevant role when streamlines patterns and the vortex characterization are concerned.

6. ACKNOWLEDGEMENTS

The authors D.D.O. Santos and L. Hermany thanks the agency CAPES for their graduate scholarships and the authors S. Frey and M.F. Naccache thanks CNPq and Petrobras for financial support.

7. REFERENCES

- Astarita, G. and Marrucci, G., 1974, "Principles of Non-Newtonian Fluid Mechanics". Vol. 1, John Wiley & Sons, U.S.A.
- Behr, M., Franca, L.P. and Tezduyar, T.E., 1993, "Stabilized Finite Element Methods for the Velocity-Pressure-Stress Formulation of Incompressible Flows", *Comput. Methods Appl. Mech. Engrg.*, Vol. 104, pp. 31-48.
- Bird, R.B., Armstrong, R. C. and Hassager, O., 1987, "Dynamics of Polymeric Liquids". Vol. 1, John Wiley & Sons, U.S.A.
- Ciarlet, P.G., 1978, "The Finite Element Method for Elliptic Problems". North Holland, Amsterdam.
- Franca, L.P., and Frey, S., 1992, "Stabilized Finite Element Methods: II. The Incompressible Navier-Stokes Equations", *Comput. Methods Appl. Mech. Eng.*, Vol. 99, pp. 209-233.
- Jay, P., Magnin, A., and Piau, J.M., 2001, "Viscoplastic Fluid Flow Through a Sudden Axisymmetric Expansion", *AIChE Journal*, vol.47, pp. 2155-2166.
- Hughes, T.J.R., Franca, L.P., and Balestra, M., 1986, "A new finite element formulation for computational fluid dynamics: V. Circumventing the Babuška-Brezzi condition: A stable Petrov-Galerkin formulation of the Stokes problem accomodating equal-order interpolations", *Comput. Methods Appl. Mech. Eng.*, Vol. 59, pp. 85-99.
- Santos, D.D.O., Frey, S.L., Naccache, M.F., and Souza Mendes, P.R., 2010, "Numerical approximations for SMD flows in a lid-driven cavity", Preprint in preparation.
- Souza Mendes, P.R., and Dutra, E.S.S., 2004, "Viscosity Function for Yield-Stress Liquids", *Applied Rheology*, Vol. 14, pp. 296-302.

- Souza Mendes, P.R., 2007, "Dimensionless non-Newtonian fluid mechanics", *J. Non-Newt. Fluid Mech.*, Vol. 147, pp. 109-116.
- Souza Mendes, P. R., Naccache, M. F., Vargas, P. R., and Marchesini, F. H., 2007, "Flow of viscoplastic liquids through axisymmetric expansions-contractions", *J. Non-Newt. Fluid Mech.*, Vol. 142, pp. 207-217.

8. RESPONSIBILITY NOTICE

The authors are the only responsible for the printed material included in this paper.